In Vivo and In Vitro Studies of Epithelial Cell Behavior around Titanium Implants with Machined and Rough Surfaces

Ikiru Atsuta, DDS, PhD;* Yasunori Ayukawa, DDS, PhD;† Akihiro Furuhashi, DDS, PhD;‡ Yoichiro Ogino, DDS, PhD;§ Yasuko Moriyama, DDS, PhD;¶ Yoshihiro Tsukiyama, DDS, PhD;** Kiyoshi Koyano, DDS, PhD††

ABSTRACT

Background: The surface roughness of a dental implant affects the epithelial wound healing process and may significantly enhance implant prognosis.

Purpose: We explored the influence of surface roughness on peri-implant epithelium (PIE) sealing and down-growth by comparing machine-surfaced (Ms) and rough-surfaced (Rs) implants.

Materials and Methods: (1) Maxillary first molars were extracted from rats and replaced with Ms or Rs implants. (2) We also compared changes in the morphology of cultured rat oral epithelial cells (OECs) grown on Ms or Rs titanium (Ti) plates.

Results: (1) After 4 weeks, the PIE around Ms and Rs implants showed a similar structure to junctional epithelium (JE). At 16 weeks, Rs implants appeared to form a weak epithelial seal at the tissue-implant interface and exhibited markedly less PIE down-growth than Ms implants but was deeper than that observed in natural teeth. (2) We observed less expression of adhesion proteins in OECs cultured on Rs plates than in cells grown on Ms plates. Additionally, cell adherence, migration, and proliferation on Rs plates were lower, whereas apoptosis was reduced on Ms plates.

Conclusion: Ms implants are a better choice for integration with an epithelial wound healing process.

KEY WORDS: adhesion molecule, dental implant, epithelial cell, surface roughness, titanium

*Assistant professor, Section of Implant and Rehabilitative Dentistry, Division of Oral Rehabilitation, Faculty of Dental Science, Kyushu University, Fukuoka, Japan, and Center for Craniofacial Molecular Biology, University of Southern California School of Dentistry, Los Angeles, California, USA; †assistant professor, Section of Implant and Rehabilitative Dentistry, Division of Oral Rehabilitation, Faculty of Dental Science, Kyushu University, Fukuoka, Japan; ‡clinical fellow, Section of Implant and Rehabilitative Dentistry, Division of Oral Rehabilitation, Faculty of Dental Science, Kyushu University, Fukuoka, Japan; §assistant professor, Section of Implant and Rehabilitative Dentistry, Division of Oral Rehabilitation, Faculty of Dental Science, Kyushu University, Fukuoka, Japan; ¶assistant professor, Section of Implant and Rehabilitative Dentistry, Division of Oral Rehabilitation, Faculty of Dental Science, Kyushu University, Fukuoka, Japan; **associate professor, Section of Implant and Rehabilitative Dentistry, Division of Oral Rehabilitation, Faculty of Dental Science, Kyushu University, Fukuoka, Japan; ††professor, Section of Implant and Rehabilitative Dentistry, Division of Oral Rehabilitation, Faculty of Dental Science, Kyushu University, Fukuoka, Japan

Reprint requests: Dr. Ikiru Atsuta, Section of Implant and Rehabilitative Dentistry, Division of Oral Rehabilitation, Faculty of Dental Science, Kyushu University, 3-1-1 Maidashi, Higashi-ku, Fukuoka 812-8582, Japan; e-mail: atyuta@dent.kyushu-u.ac.jp

DOI 10.1111/cid.12043

INTRODUCTION

Dental implant treatment is an important prosthodontic option for treating patients that are completely or partially edentulous. These implants draw on the concept of "osseointegration," a term coined by Brånemark in the 1960s to describe the fixation of a titanium implant into bone.[1] There have been continuous advances in implant technology since then including developments in the science of implant surface topography, with various novel surface treatment techniques introduced to improve the stability and biological acceptance of titanium implants.[2–4] Rough surfaces have been shown to allow greater proportions of cell attachment and molecular adhesion.[5,6] This, in turn, induces better bone tissue formation around the implant, and therefore, suitable osseointegration.[7]

However, the success of these rough-surfaced (Rs) implants in the long term remains controversial. The soft tissues (i.e., epithelial and connective tissues)

are also important considerations for implant success because the oral mucosa is penetrated by the implant and therefore presents a risk of inflammation in the peri-implant tissue.[8] Furthermore, in vivo findings have indicated that rough surfaces inhibit maturation of the soft tissues encircling the implant.[6] Accordingly, there is some debate about the implications of surface roughness in mucosal attachment to titanium implants.

The interface between the implant and the bone is sealed off from the oral cavity by the peri-implant epithelium (PIE) to protect the jaw bone from bacteria. The PIE attaches to the implant surface by the basement membrane (BM) *via* hemidesmosomes, which are adhesion plaques in the plasma membrane of epithelial cells that adhere to the extracellular matrix.[9] HDs are multiprotein complexes,[10] among which laminin (Ln)-5, integrin α6β4, and plectin are particularly important constituents. Thus, the epithelium-implant interface has both defense elements and bonding mechanical closures.[11] Bacteria, however, readily accumulate around the implant circumference and often cause inflammation, inducing destruction similar to that observed with the natural tooth (Nt).[12] This destruction creates a pocket around the implant due to epithelial down-growth at the soft tissue-implant interface, providing a path of ingress for external bacteria to penetrate deep into the tissue, which threatens to damage the collagenous tissue, decrease the supporting bone around the implant, and precipitate implant failure.[13] Consequently, it is critical to limit epithelial down-growth by promoting strong epithelial and connective tissue seals.

In this study, we evaluated the relationship between epithelial cells and machine-surfaced (Ms) or Rs titanium implants with in vivo and in vitro experiments. We aimed to clarify whether a machined surface on a titanium implant supports epithelial attachment structures to a greater or lesser degree than a roughened surface. Our results lead us to speculate that Ms is a more suitable surface property than Rs for the part of the implant penetrating through the oral mucosa.

MATERIALS AND METHODS

Implants

We evaluated two types of screw-type pure titanium implant (Japan Industrial Standards Class 1; equivalent to ASTM grade 1): Ms and Rs (Sky Blue, Fukuoka, Japan), each measuring 4 mm in length and 2 mm in diameter (Figure 1), similar to previously described designs.[11,14] The surface analysis (Sa) of the Ms and Rs implants was performed using an electron beam three-dimensional surface roughness analyzer (ERA-8900, Elionix, Tokyo, Japan). The Sa of Ms and Rs was 0.16 μm and 0.25 μm, respectively.[15] Rats were kept according to the ethical guidelines for animal care established by the Kyushu University ethics committee (approval number: A21-237-0). Surgical implantation was performed as described previously.[11,16] In brief, the maxillary right first molars of 6-week-old Wistar rats (20 males, 120–150 g) were extracted under systemic chloral hydrate and local lidocaine hydrochloride anesthesia and the experimental implant screwed into the cavity. Following

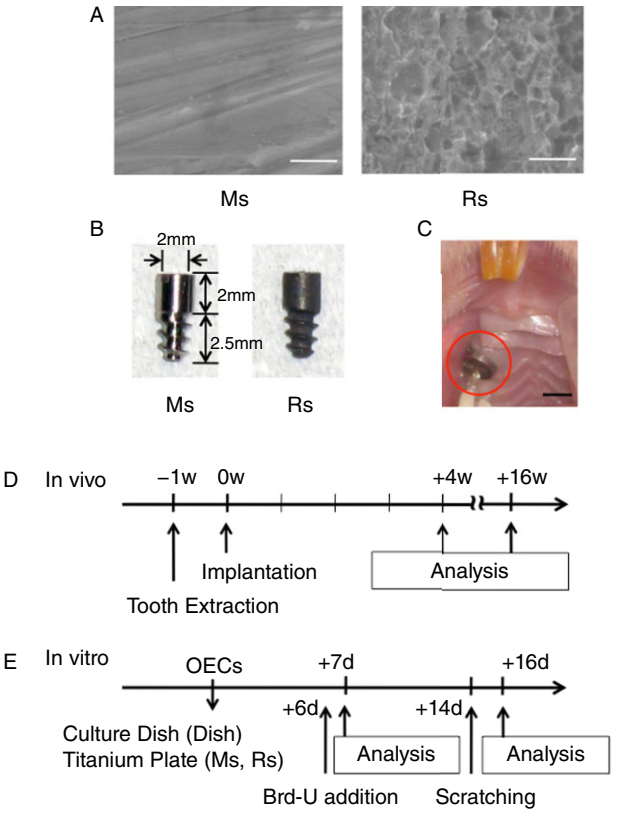

Figure 1 Experimental design for machine-surfaced (Ms) and rough-surfaced (Rs) implants. (A) SEM image of Ms and Rs titanium plates (bar = 3 μm). (B) Photograph of Ms and Rs implants. (C) Photograph of the implant in the rat oral cavity. There is no apparent inflammation in the oral mucosa around the implant (bar = 2 mm). (D) Experimental protocol of in vivo study. Implantation was performed 1 week after tooth extraction. The structure of epithelial tissue around the tooth or implant was observed after 4 or 16 weeks. (E) Experimental protocol of in vitro study. Rat oral epithelial cells (OECs) were analyzed for changes in cell morphology 7 or 14 days after seeding OECs onto control, Ms or Rs plates.

surgery, rats were treated with buprenorphine (0.05 mg/kg intramuscular injection) to alleviate any postoperative pain.

Tissue Preparation and Immunohistochemistry

Tissue preparation was performed as described previously.[9] Rats were sacrificed at various time points, and their maxillae were removed and immersed in 4% paraformaldehyde for 24 h then in 5% ethylenediaminetetraacetate solution for 4 days at 4°C. Samples of oral mucosa were carefully removed and snap frozen before being embedded in 20% sucrose overnight at 4°C, immersed in O.C.T. compound (Sakura Finetek, Tokyo, Japan) for 2 h at 4°C, and finally cut into 6 μm-thick bucco-palatal sections using a cryostat at −20°C. For immunohistochemistry, sections were blocked for 30 min with 10% normal goat serum and incubated overnight with polyclonal rabbit Ln-5 IgG (Clone 2778; provided by Dr. Vito Quaranta, The Scripps Research Institute, La Jolla, CA; 1:100) at 4°C, followed by biotinylated goat anti-rabbit IgG (1:200) for 45 min, and visualized with ABC-DAB procedure (Vector Laboratories, Bulingame, CA, USA). Sections were counterstained lightly with hematoxylin, and images were captured using a light microscope.

Biomaterials for In Vitro Experiments

Pure titanium plates (15 mm diameter; 1 mm-thick; Japan Industrial Specification H 4600, 99.9 mass%) modified with either Ms or Rs treatment were compared with polystyrene culture dishes (Cont) (Falcon Labware, Franklin Lakes, NJ, USA). The surface topographies of Ms plates were determined using a profilometer (Handy Surf E-30A; Tokyo Seimitsu, Tokyo, Japan). Rs plates were produced from Ms plates as described previously.[15] Briefly, Ms plates were grit-blasted using alumina powder (particle size ~50 μm), and the oxide layer was removed from the surface by placing plates in a 15% solution of HF at room temperature for 30 s. Plates were then removed from the hydrogen fluoride solution, neutralized, and then placed into an etch solution consisting of a 2:1 mixture of 95.5% H_2SO_4 and 31.45% HCl at room temperature for 3 min. The plates were then neutralized again, rinsed, and cleaned. The surface roughness of Ms and Rs was measured as described above, and the surface analysis was calculated to be 0.12 μm and 0.26 μm, respectively.

Cell Culture

Rat oral epithelial cell (OEC) cultures were created as described.[17] Briefly, the oral mucosa from 4-day-old Wistar rats was incubated with dispase (1×10^3 IU/mL) in Mg^{2+}- and Ca^{2+}-free Dulbecco's phosphate-buffered saline (PBS) for 12 h at 4°C and removed from the connective tissue. Cells were cultured in Defined Keratinocyte Serum Free Medium (DK-SFM; Invitrogen, Grand Island, NY, USA) in culture dishes, or on Ms or Rs titanium plates in a humidified atmosphere of 95% air and 5% CO_2 at 37°C.

Adhesion Assays

Adhesion assays of OECs were performed as described in our previous report.[18] Briefly, nonadherent cells were removed by three periods of shaking at 75 rpm for 5 min in DK-SFM using a rotary shaker (NX-20, Nissin, Tokyo, Japan). The proportion of cells remaining (i.e., the adherent cell population) was expressed as a percentage of the total count, and this value was used to define the adherence capacity of the cells.

Immunofluorescence Staining for Adhesion Proteins

OECs cultured on Ms or Rs plates or Cont were fixed in 4% paraformaldehyde for 10 min. For fluorescence staining, samples were treated in 0.5% (V/V) Triton X-100 (Novocastra Laboratories Ltd., Newcastle, UK) for 3 min, blocked with 10% normal goat serum for 30 min at 37°C, and incubated overnight at 4°C with anti-rat Ln-5 (Clone 2778; 1:100), anti-rat In-β4, or anti-rat plectin polyclonal antibodies (Chemicon International Inc. Temecula, CA, USA; 1:100). Samples were incubated with TRITC- or FITC-conjugated secondary antibodies for 2 h at 37°C. Actin filament staining was carried out using TRITC-conjugated phalloidin (Sigma Chemical Co., Balcatta, WA, Australia; 1:100) for 1 h at 37°C. Imaging was performed using an Axiotech Microscope (Carl Zeiss, Göttingen, Germany).

Western Blot Analysis

Proteins were separated by 7.5% SDS-PAGE then transferred to polyvinylidene difluoride membranes (Bio-Rad Laboratories, Hercules, CA, USA) and immunoblotted with In-β4 (1:100) or plectin (1:100) antibodies for 24 h at 4°C. Membranes were then incubated with the secondary antibody, horseradish peroxidase-conjugated

anti-rabbit IgG (GE Healthcare, Little Chalfont, UK) for 1 h and processed using ECL semidry blotters (GE Healthcare).

Wound Healing Assays (Scratch Assays)

Scratch assays on confluent monolayers of OECs were carried out as models for control wounds on Ms and Rs plates and Cont, as previously described.[19]

Apoptosis Analyses

OECs were seeded onto Ms or Rs plates or Cont and incubated for 6 days. Cells were switched to serum-free medium for 24 h, harvested, washed in PBS, and incubated with Annexin-V-FITC and 7AAD-PerCP for 15 min in the dark. Apoptosis was analyzed on a FACS-Calibur instrument (BD Biosciences Ltd., Franklin Lakes, NJ, USA) as described previously.[20]

Proliferation Analyses

Cell proliferation was quantified using a cell proliferation kit (GE Healthcare). OECs were exposed to 5-bromo-2′-deoxyuridine (BrdU) in the culture medium for 24 h, fixed in 70% methanol for 30 min and then incubated with anti-BrdU antibody for 1 h. Cells were then incubated with FITC-conjugated anti-mouse IgG (Molecular Probes, Eugene, OR, USA) (1:100) and were counted.

Statistical Analysis

Data are expressed as mean ± standard deviation. One-way analysis of variance with Fisher's least significant difference tests was performed. Values of $p < .05$ were considered to be statistically significant. Experiments were performed using triplicate samples and at least two independent repeats to verify the reproducibility of the results.

RESULTS

Laminin-5 Localization

OECs growing on tissue culture dishes (Cont) showed numerous punctate Ln-5 signals (Figure 2A). In addition, diffusely scattered signals were observed in the direction of cell movement. Actin filaments were localized just beneath the cell membrane, and the leading edge of the cell had small but numerous lamellipodia. Histology revealed an immunoreactive band of Ln-5 along the dento-junctional epithelium (JE) interface

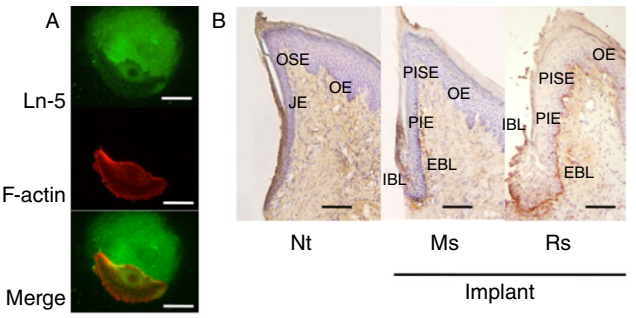

C Location and strength of Ln-5

		Nt	Implant	
			Ms	Rs
OE		–	–	+
OSE		–	±	++
PIE (JE)	IBL	+	+	++
	EBL	±	+	++

Figure 2 *A*, Expression of Laminin-5 (in vitro). OECs were cultured for 7 days in culture dishes. Green and red staining denotes Ln-5 and actin filaments, respectively (bar = 20 μm). *B*, Structure of junctional or peri-implant epithelium (PIE) in vivo. Light micrographs of Ln-5 distribution in the gingiva around natural tooth (Nt) and machine-surfaced (Ms) or rough-surfaced (Rs) implants after 4 weeks. IBL and EBL are the internal and external basement lamina, respectively (bar = 200 μm). *C*, Laminin-5 expression. Data shown for intensity of Ln-5 expression derived from immunohistochemistry data (panel b). Expression level is annotated as: ++, strong; +: positive, ±: weak, –: negative.

(see Figure 2B; Nt). In addition, positive, albeit weaker, Ln-5 staining was detected along the JE-connective tissue interface. Almost no Ln-5 was noted in the BM underlying either the oral sulcular epithelium (OSE) or the oral epithelium (OE) (see Figure 2, C and D).

The pattern of Ln-5 deposition at the interface between the PIE and the Ms implant (see Figure 2B; Ms) was noticeably different from that in the JE of Nt. Ln-5-positive staining on the Ms implant was apparent as a band along the implant-PIE interface but was not evident along the majority of the upper portion of the interface. In the Rs implant (see Figure 2B; Rs), a few structural differences were noted, with significantly thicker PIE in the Rs implant than in the Nt and Ms implant. Moreover, the keratinized stratum corneum and the OE penetrated the space surrounding the Rs implant more deeply than in the other groups. However, the majority of Ln-5 immunoreactivity was located in the lower portion and at the OSE- and OE-connective tissue interfaces, with little in the upper portion (see Figure 2C). The positive staining pattern for Ln-5 on the

Rs implant in the BM underlying both the OSE and the OE was much stronger than on the Ms implant (see Figure 2D). There was no Ln-5 immunoreactivity in either of the negative controls for the natural gingiva and the oral mucosa (results not shown).

Expression and Distribution of Adhesion-Related Proteins

The OECs on culture dishes (Cont) and Ms plates contained punctate In-β4 deposits throughout the cytoplasm, whereas on Rs plates In-β4 accumulated around the nucleus. Plectin showed intense focal signals in the cytoplasm (Figure 3A). The distribution pattern in the OECs on the Ms plates was similar to those on Cont, but few assemblies were observed on the Rs plates. All substrata showed positive actin filament staining at the intracellular margins of the cells. However, the filaments in the OECs on Ms and Rs plates had many interruptions. In addition, the OECs on Rs plates had less developed filaments than those on the Ms plates. Western blotting showed that the expression levels of In-β4 and plectin on Ms were slightly weaker than those in the Cont, whereas the expression of these proteins in OECs was much lower on Rs plates than on Cont or Ms plates (see Figure 3B). Overall, these results corroborate the findings observed with immunofluorescence.

Cell Adhesion and Migration

Cell adhesion to the Ms plates was significantly lower than in the Cont group (see Figure 3C) and was even lower in the Rs plates. The number of cells migrating from the edge on the Ms plate was significantly higher than the other groups (Figure 4A, left) and the OECs located distally to the wound area. There was little evidence of cell motility on Rs plates, notably less than on the Ms plates, but still more than in the Cont group. The right panels in Figure 4 show typical images of the leading front of the epithelial sheet, demonstrating the OEC lamellipodia. In the Cont group, actin filaments extended into the lamellipodia from actin bundles that seemed to shape the cytoskeleton. However, this was not observed on either of the titanium surfaces, as most of the cells from the wound edge had already started moving toward the wound area.

Cell Apoptosis and Proliferation

The prevalence of apoptotic OECs in the Cont group was 1.86%, whereas that in the Ms and Rs groups was 11.24%

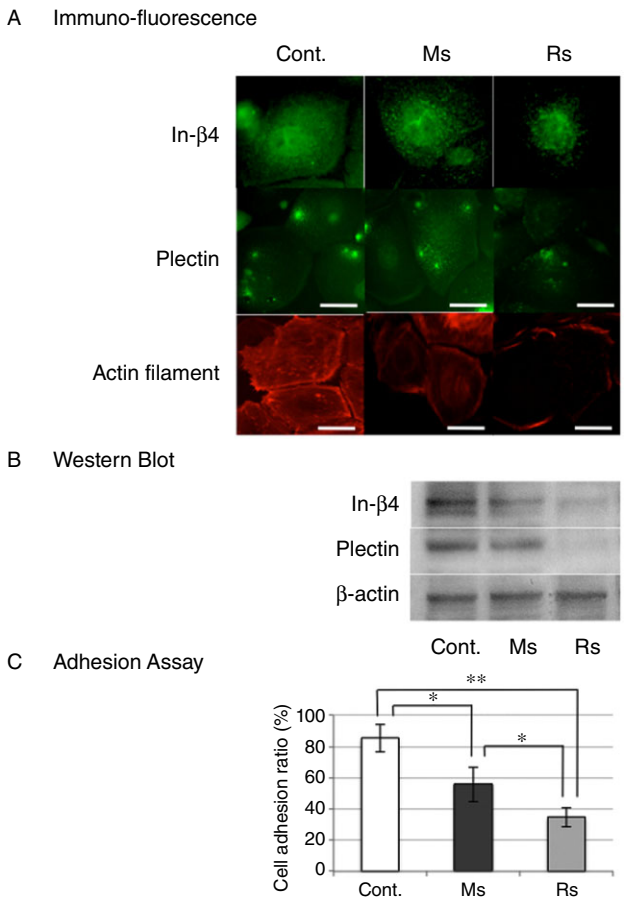

Figure 3 Adhesion of oral epithelium cells. (A) Localization of actin, In-β4, and plectin proteins in oral epithelial cells (OECs) after 1 week of culture on culture dishes (Cont) and machine-surfaced (Ms) or rough-surfaced (Rs) plates (bar = 15 μm). (B) Western blot analyses of actin, In-β4, and plectin protein expression. (C) Adhesion assay. The adhesive potential of cells to Ms, Rs, and Cont plates after 1 week in culture was tested using a shaking-based detachment assay. The bars indicate the cell adhesion ratio of OECs to the culture dishes (Cont; white bar), titanium plates with Ms (black bar), and those with Rs (gray bar). Bars represent the mean ± SD of three independent experiments. $^{*}p < .05$, $^{**}p < .01$.

and 16.32%, respectively (see Figure 4B), indicating that apoptosis on titanium was very high. The number of BrdU-positive cells was also determined (see Figure 4C) and found to be significantly lower on Ms plates than in the Cont group and lower still on the Rs plates.

PIE Down-Growth around Implants

Changes in the JE and PIE were examined in each group 16 weeks after implantation. Using light microscopy (Figure 5A), we identified no significant changes to the JE. In contrast, the PIE in both the Ms and Rs groups showed an obvious change, with Ln-5 being diffusely scattered in the connective tissue of the apical portion

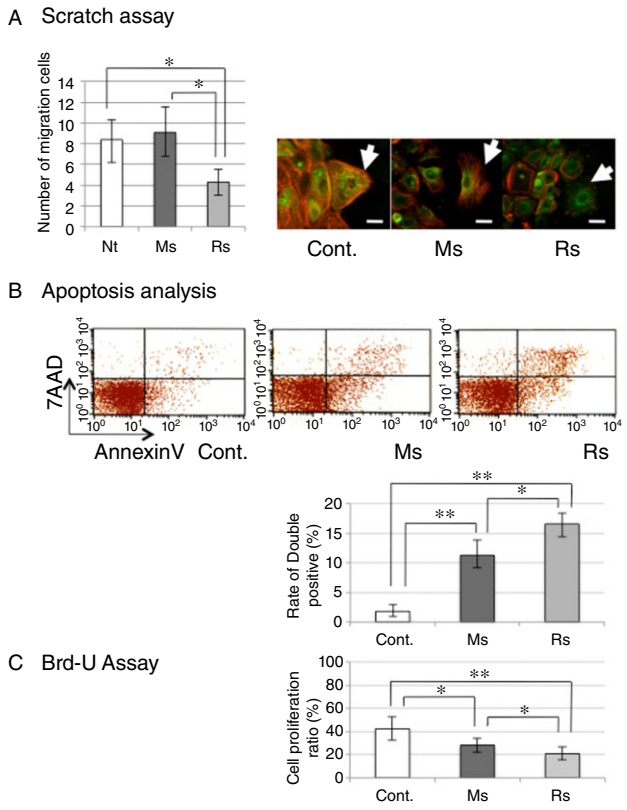

Figure 4 Phenotypic analyses of cells. (A) Scratch assay. Oral epithelium cells were cultured for 2 weeks on culture dishes (Cont.; white bar) or titanium plates (Ms: black bar; Rs: gray bar). OEC numbers were determined 96 h after scratching (left table). Rs had significantly smaller numbers of migrating cells than Ms (right panels). Each data point represents the mean ± SD of three independent experiments. $^{*}p < .05$, $^{**}p < .01$. (B) OEC migration was tracked using immunofluorescence staining (right panels). White arrows denote migratory cells. Actin filaments are indicated by red staining, whereas green staining indicates integrin β4. (bar = 15 μm). (B) Apoptosis analysis. OECs were grown on culture dishes (Cont) or titanium plates (Ms, Rs) for 1 week before being harvested. Apoptotic cells were detected and quantified using a fluorescence-activated cell sorting procedure. Upper panels show raw FACS data, lower panels show processed data from the same experiments. Data points represent the mean ± SD of three independent experiments. $^{*}p < .05$, $^{**}p < .01$. (C) BrdU assay. The percentage of OECs grown on culture dishes (Cont) and titanium plates (Ms, Rs) after 7 days that are actively proliferating was calculated using a BrdU incorporation assay. Bars represent the mean ± SD of three independent experiments. $^{*}p < .05$, $^{**}p < .01$.

of the PIE. In addition, Ln-5 expression at the PIE-connective tissue interface was more intense at 16 weeks than at 4 weeks. The keratinized stratum corneum and the OE moved into the space surrounding most of the implants. Interestingly, the PIE around the Rs implant was significantly thicker than around the Ms implant. No down-growth of the JE was observed in the Nt group (see Figure 5B). However, apical movement of the PIE was observed for most implants at 16 weeks. The Rs implant appeared to inhibit PIE down-growth on the implant surface.

DISCUSSION

The efficacy of dental implants and the risk of associated infections are both linked to the achievement of a tight epithelial attachment between the implant and the PIE. Here, we compared the effects of Ms and Rs implant topography on the extent and strength of this attachment and demonstrated that an implant with a machined surface offers superior availability for attachment of the epithelial layer.

Contact between the PIE and Rs Implants

For most RS dental implants, osseointegration is customary. However, despite being physically interfaced with alveolar bone immediately after placement, these surfaces often come into contact with the mucosa and epithelial tissue because of subsequent bone resorption,[21,22] and the implant-abutment interface therefore often becomes the origin of inflammation.[23,24] The "biologic width" is an estimate of the distance between the junctional epithelium and connective tissue attachment to the root surface[22] (Figure 6). Bone exposed to the oral cavity will always cover itself with epithelium and connective tissue. If a chronic irritant, such as bacteria, reaches the implant-abutment junction, the bone will be resorbed to increase the biologic width between it and the infection (Figure 7).[25,26] To prevent this from happening, the soft tissues that seal the implant site from bacterial invasion need to attach to the implant body

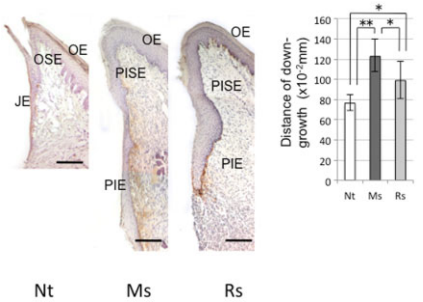

Figure 5 Down-growth of PIE on the implant. (A) Light micrographs of the PIE around the natural tooth (Nt) and machine-surfaced (Ms) or rough-surfaced (Rs) implants at 16 weeks after implantation. Bar = 200 μm. (B) Average PIE down-growth in the Nt, Ms, and Rs groups. Data are mean ± SD of three independent experiments. $^{*}p < .05$, $^{**}p < .01$.

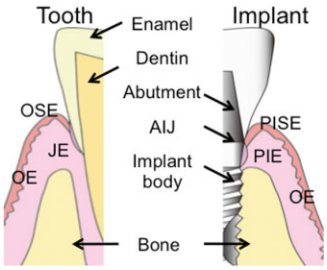

Figure 6 Structure of the gingiva. Schematic diagram of the gingiva surrounding the tooth (left) and dental implant (right). Abbreviations: OE, oral epithelium; OSE, oral sulcural epithelium; PISE, peri-implant sulcural epithelium; JE, nonkeratinized junctional epithelium; PIE, peri-implant epithelium. AIJ refers to the abutment-implant body junction, the interface between the implant abutment and the implant body.

surface, but their ability to do so is influenced by the texture of the titanium surface. Consequently, we explored the relationship between the PIE and the implant body surface.

PIE Characteristics When Interfaced with a Rough Titanium Surface

Generally, the keratinized layer of OE is thick, whereas the keratinized layers of OSE and peri-implant sulcural epithelium (PISE) are thin, making it easy to distinguish OSE from OE.[27] However, around Rs implants, the PISE and PIE were much thicker than in other groups (see Figure 2b), and PIE also exhibits a strong positive signal for Ln-5, detected as a diffuse band from the PIE to the connective tissue (see Figure 2, B–D), in agreement with our previous findings.[14] In contrast, the OE showed strong Ln-5 expression deep into the pocket surrounding the implant. These data suggest that, despite less down-growth of PIE around the Rs implant surface, the epithelial cells in this layer are not as stable. As a consequence, the PIE surrounding the Rs implant may be incomplete at 4 weeks and still in the process of wound healing.

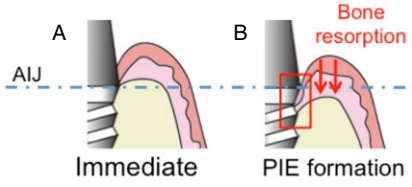

Figure 7 Temporal changes in adjacent tissues. Images showing the implant height relative to the adjacent alveolar bone level immediately postsurgically (A) and some time after (B) surgical placement of the implant. The blue dotted line denotes the abutment-implant body junction (AIJ). Red arrows indicate areas where bone resorption has created a "biologic width"-like structure with epithelial and connective tissue sealing (demarcated by the red square).

Adhesion Proteins

We investigated the distribution of adhesion molecules by fluorescence staining for OECs grown on Ms and Rs plates and compared this to tissue culture plastic (Cont). Overall, we saw no differences in Ln-5 expression between the three substrates. Similarly, numerous intracellular punctate signals of In-β4 were observed on all materials, supporting previous findings with human bronchial epithelial cells.[28] Plectin localization was also consistent with a previous report on primary mouse fibroblasts, showing patches of staining at the cell periphery and in the whole cell body.[29] However, plectin expression by cells grown on titanium was lower than those grown on the Cont surface, with Rs plates showing the lowest expression overall. This low expression of adhesion molecules on titanium may be the result of a lack of bioactive coatings that are commonly found on culture dishes, or could be due to differences in surface charge or liquation.[17,30,31] Moreover, there was weakness of the actin filaments in these cells; the development of actin filaments is influenced by the expression of integrins[32] or plectin distribution.[33] The microgrooved titanium had a high population density and parallel alignment of fibroblasts along the groove, and these cells exhibited much higher and earlier adhesion to microgrooved titanium than to normal titanium.[15] However, cells on titanium with Rs appeared to be less amenable to cell alignment and therefore produced weaker epithelial cell adhesion.

Migration of OECs on Titanium with Rough Surface

Wound closure rates in scratch assays are affected by both the migration of leading cells and the proliferation of following cells.[34] In this study, the OECs on Ms plates migrated over longer distances than cells on Rs plates, even though cell attachment was superior on Ms plates. This result is contradictory to the view that cell-substrate attachment is important for subsequent cell spreading and proliferation.[35] We suggest two reasons for this discrepancy: (1) Rs plates may simply have a larger surface area than Ms plates and (2) the shape of the Rs plates may block cell migration by preventing the

formation of focal adhesions that are important for cell migration, as previously reported.[17,36]

Apoptosis of OECs on Titanium with a Rough Surface

Most dental implants are made from titanium because it is insoluble in the oral cavity. However, it is not completely stable. Epidermal cells in contact with TiO_2 particles can potentially produce epidermal interactions and toxicity.[37] In this study, Ti may have influenced OEC apoptosis. Furthermore, the difference in apoptosis between the OECs on Ms and Rs plates may be due to different adherence levels, as cellular adhesion has been shown to inhibit apoptosis in many cell lines. For example, blocking cell contact and downregulating cell adhesion molecules, such as integrin and intercellular adhesion molecule 1, can induce apoptosis.[38]

Proliferation of OECs on Titanium with Rough Surface

Here, we observed slower rates of proliferation for cells seeded onto Rs plates. Wang and colleagues also showed slower rates of proliferation for human skin epithelium on microarc oxidation-treated titanium, which has a rough surface.[36] Moreover, we previously showed faster proliferation of rat fibroblasts on polished titanium than on titanium that had been blasted and etched.[15] This difference may also be due to lower cell adhesion levels.

Down-Growth around the Implant with Rough Surface

After 16 weeks, we noted apical down-growth of the PIE and marked spreading deposition of Ln-5 from the apical edge of the PIE to the connective tissue around our experimental implants. The distance of PIE migration on Rs implants was shorter than on Ms implants, consistent with the in vitro data. However, these results are inconsistent with previous clinical reports showing that Rs implants caused deep pockets.[6] We speculate that osseointegration between the jaw bone and the Rs implant delayed this apical movement. However, expression of Ln-5 in PIE cells around Rs implants was much higher than in those around Ms implants. The PIE around Rs implants seemed unstable, as described above, and was possibly inclined to migrate because the cells at the apical edge of the PIE secreted high levels of Ln-5.

CONCLUSIONS

The PIE around the Rs implant was incomplete in the time point studied here so it could not promote apical down-growth. Additionally, the Rs implant employed in the present study appears to show weaker epithelial sealing than the Ms implant, as the adhesion of epithelial cells to Rs plates was very weak. Thus, in terms of epithelial suitability in the present study, Ms implants are more appropriate than Rs implants for successful wound healing. Therefore, we suggest that an implant with a machined surface on the supra-bony portion (and any part that may become supra-bony following bone resorption) is advantageous in achieving a high-quality epithelial seal.

ACKNOWLEDGMENT

This work was supported by a grant-in-aid for Scientific Research (C) no. 23592888 (to I. Atsuta) from the Ministry of Education, Culture, Sports, Science and Technology of Japan.

REFERENCES

1. Brånemark PI, Adell R, Albrektsson T, Lekholm U, Lundkvist S, Rockler B. Osseointegrated titanium fixtures in the treatment of edentulousness. Biomaterials 1983; 4: 25–28.
2. Chehroudi B, Gould TR, Brunette DM. A light and electron microscopic study of the effects of surface topography on the behavior of cells attached to titanium-coated percutaneous implants. J Biomed Mater Res 1991; 25:387–405.
3. Eisenbarth E, Meyle J, Nachtigall W, Breme J. Influence of the surface structure of titanium materials on the adhesion of fibroblasts. Biomaterials 1996; 17:1399–1403.
4. Mustafa K, Silva Lopez B, Hultenby K, Wennerberg A, Arvidson K. Attachment and proliferation of human oral fibroblasts to titanium surfaces blasted with TiO2 particles. A scanning electron microscopic and histomorphometric analysis. Clin Oral Implants Res 1998; 9:195–207.
5. Ellingsen JE, Thomsen P, Lyngstadaas SP. Advances in dental implant materials and tissue regeneration. Periodontol 2000 2006; 41:136–156.
6. Wennerberg A, Sennerby L, Kultje C, Lekholm U. Some soft tissue characteristics at implant abutments with different surface topography. A study in humans. J Clin Periodontol 2003; 30:88–94.
7. Orsini G, Assenza B, Scarano A, Piattelli M, Piattelli A. Surface analysis of machined versus sandblasted and acid-etched titanium implants. Int J Oral Maxillofac Implants 2000; 15:779–784.

8. Albrektsson TO, Johansson CB, Sennerby L. Biological aspects of implant dentistry: osseointegration. Periodontol 2000 1994; 4:58–73.
9. Ikeda H, Yamaza T, Yoshinari M, et al. Ultrastructural and immunoelectron microscopic studies of the peri-implant epithelium-implant (Ti-6Al-4V) interface of rat maxilla. J Periodontol 2000; 71:961–973.
10. Borradori L, Sonnenberg A. Hemidesmosomes: roles in adhesion, signaling and human diseases. Curr Opin Cell Biol 1996; 8:647–656.
11. Atsuta I, Yamaza T, Yoshinari M, et al. Ultrastructural localization of laminin-5 (gamma2 chain) in the rat peri-implant oral mucosa around a titanium-dental implant by immuno-electron microscopy. Biomaterials 2005; 26: 6280–6287.
12. Ikeda H, Shiraiwa M, Yamaza T, et al. Difference in penetration of horseradish peroxidase tracer as a foreign substance into the peri-implant or junctional epithelium of rat gingivae. Clin Oral Implants Res 2002; 13:243–251.
13. Berglundh T, Gotfredsen K, Zitzmann NU, Lang NP, Lindhe J. Spontaneous progression of ligature induced peri-implantitis at implants with different surface roughness: an experimental study in dogs. Clin Oral Implants Res 2007; 18:655–661.
14. Atsuta I, Yamaza T, Yoshinari M, et al. Changes in the distribution of laminin-5 during peri-implant epithelium formation after immediate titanium implantation in rats. Biomaterials 2005; 26:1751–1760.
15. Furuhashi A, Ayukawa Y, Atsuta I, Okawachi H, Koyano K. The difference of fibroblast behavior on titanium substrata with different surface characteristics. Odontology 2012; 100:199–205.
16. Atsuta I, Ayukawa Y, Ogino Y, Moriyama Y, Jinno Y, Koyano K. Evaluations of epithelial sealing and peri-implant epithelial down-growth around "step-type" implants. Clin Oral Implants Res 2012; 23:459–466.
17. Shiraiwa M, Goto T, Yoshinari M, Koyano K, Tanaka T. A study of the initial attachment and subsequent behavior of rat oral epithelial cells cultured on titanium. J Periodontol 2002; 73:852–860.
18. Yan T, Sun R, Deng H, Tan B, Ao N. The morphological and biomechanical changes of keratocytes cultured on modified p (HEMA-MMA) hydrogel studied by AFM. Scanning 2009; 31:246–252.
19. Li Y, Lin JL, Reiter RS, Daniels K, Soll DR, Lin JJ. Caldesmon mutant defective in Ca(2+)-calmodulin binding interferes with assembly of stress fibers and affects cell morphology, growth and motility. J Cell Sci 2004; 117:3593–3604.
20. Métrailler-Ruchonnet I, Pagano A, Carnesecchi S, Ody C, Donati Y, Barazzone Argiroffo C. Bcl-2 protects against hyperoxia-induced apoptosis through inhibition of the mitochondria-dependent pathway. Free Radic Biol Med 2007; 42:1062–1074.
21. Berglundh T, Lindhe J. Dimension of the periimplant mucosa. Biological width revisited. J Clin Periodontol 1996; 23:971–973.
22. Cochran DL, Hermann JS, Schenk RK, Higginbottom FL, Buser D. Biologic width around titanium implants. A histometric analysis of the implanto-gingival junction around unloaded and loaded nonsubmerged implants in the canine mandible. J Periodontol 1997; 68:186–198.
23. Grunder U. Stability of the mucosal topography around single-tooth implants and adjacent teeth: 1-year results. Int J Periodontics Restorative Dent 2000; 20:11–17.
24. Tarnow DP, Wallace SS, Froum SJ, Rohrer MD, Cho SC. Histologic and clinical comparison of bilateral sinus floor elevations with and without barrier membrane placement in 12 patients: part 3 of an ongoing prospective study. Int J Periodontics Restorative Dent 2000; 20:117–125.
25. Jansen VK, Conrads G, Richter EJ. Microbial leakage and marginal fit of the implant-abutment interface. Int J Oral Maxillofac Implants 1997; 12:527–540.
26. Tarnow D, Stahl SS, Magner A, Zamzok J. Human gingival attachment responses to subgingival crown placement. Marginal remodelling. J Clin Periodontol 1986; 13:563–569.
27. Schroeder HE. Healing and regeneration following periodontal treatment. Dtsch Zahnarztl Z 1986; 41:536–538.
28. Michelson PH, Tigue M, Jones JC. Human bronchial epithelial cells secrete laminin 5, express hemidesmosomal proteins, and assemble hemidesmosomes. J Histochem Cytochem 2000; 48:535–544.
29. Sieg DJ, Hauck CR, Schlaepfer DD. Required role of focal adhesion kinase (FAK) for integrin-stimulated cell migration. J Cell Sci 1999; 112(Pt 16):2677–2691.
30. Diener A, Nebe B, Luthen F, et al. Control of focal adhesion dynamics by material surface characteristics. Biomaterials 2005; 26:383–392.
31. Eisenbarth E, Velten D, Schenk-Meuser K, et al. Interactions between cells and titanium surfaces. Biomol Eng 2002; 19:243–249.
32. Chu CL, Reenstra WR, Orlow DL, Svoboda KK. Erk and PI-3 kinase are necessary for collagen binding and actin reorganization in corneal epithelia. Invest Ophthalmol Vis Sci 2000; 41:3374–3382.
33. Rezniczek GA, Janda L, Wiche G. Plectin. Methods Cell Biol 2004; 78:721–755.
34. Nobes CD, Hall A. Rho GTPases control polarity, protrusion, and adhesion during cell movement. J Cell Biol 1999; 144: 1235–1244.
35. Okumura A, Goto M, Goto T, et al. Substrate affects the initial attachment and subsequent behavior of human osteoblastic cells (Saos-2). Biomaterials 2001; 22: 2263–2271.

36. Wang XJ, Maier K, Fuse S, et al. Thrombospondin-1-induced migration is functionally dependent upon focal adhesion kinase. Vasc Endovascular Surg 2008; 42:256–262.
37. Lademann J, Weigmann H, Rickmeyer C, et al. Penetration of titanium dioxide microparticles in a sunscreen formulation into the horny layer and the follicular orifice. Skin Pharmacol Appl Skin Physiol 1999; 12:247–256.
38. Roehlecke C, Kuhnt AK, Fehrenbach H, Werner C, Funk RH, Kasper M. Resistance of L132 lung cell clusters to glyoxal-induced apoptosis. Histochem Cell Biol 2000; 114:283–292.